

# **CHAPTER - II**

## **Experimental Procedures and Characterization Techniques**

# Chapter-II

## Experimental Procedures and Characterization Techniques

### 2.1. Introduction

Materials in the nanometre scale have been studied over many years and many physical properties related to the nanometre size, such as coloration of gold nanoparticles, have been known for centuries. One of the critical challenges faced currently by researchers in the nanotechnology and nanoscience fields is the inability and the lack of instruments to observe measure and manipulate the materials at the nanometre level by manifesting at the macroscopic level. In the past, the studies have been focused mainly on the collective behaviours and properties of a large number of nanostructured materials. The properties and behaviours observed and measured are typically group characteristics. A better fundamental understanding and various potential applications increasingly demand the ability and instrumentation to observe measure and manipulate the individual nanomaterial and nanostructures. Characterization and manipulation of individual nanostructures require not only extreme sensitivity and accuracy, but also atomic level resolution. It therefore leads to various methods that will play a central role in characterization and measurements of nanostructured materials and nanostructures. Miniaturization of instruments is obviously not the only challenge; the new phenomena, physical properties and short-range forces, which do not play a noticeable role in macroscopic level characterization, may have significant impacts in the nanometre scale. The development of novel tools and instruments is one of the greatest challenges in nanotechnology.

**Characterization**, when used in materials science, refers to the use of external techniques to probe into the internal structure and properties of a material. The operations involved in nanoparticle characterization are related to their state of delivery – solid powder or liquid dispersion – and to their intended use. Main features are particle morphology, size, and size distribution. The surface area and surface chemistry are also relevant. This operation is critical and must be done in a manner which is representative for the planned use of the nanopowders.

## 2.2. Synthesis of nanomaterial using Sol-gel method

We have synthesized pure and doped BT nanocrystals through a chemical sol-gel route with two different process.

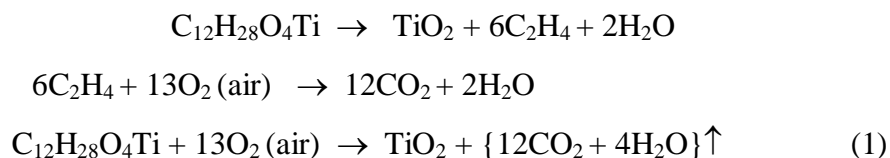
### ❖ *Method I:*

Pure BT-nanocrystals were prepared by sol-gel hydroxide method using raw chemicals  $\text{Ba}(\text{OH})_2 \cdot 8\text{H}_2\text{O}$  and tetra-isopropyl orthotitanate ( $\text{C}_{12}\text{H}_{28}\text{O}_4\text{Ti}$ ). Both the reagents were 99.9% pure and were procured from Merck chemicals.  $\text{Ba}(\text{OH})_2 \cdot 8\text{H}_2\text{O}$  was dissolved in ethanol and glacial acetic acid (1:1 volume ratio) by stirring and heating at 50-70 °C. After cooling to room temperature, tetra-isopropyl orthotitanate was admixed in the stoichiometric ratio to form BT. A transparent solution, obtained after stirring for few minutes, was allowed gelation at room temperature. BT-nanocrystals of selective sizes were formed on heating a dried gel in parts at 400-750 °C for 2 h. For the preparation of BT doped with transition metal ion, calculated amount of raw materials were taken following the general formula  $\text{Ba}(\text{Ti}_{1-x}\text{X}_x)\text{O}_3$ , where 'X' is the doping ion and 'x' the mole % of the doping ion. We took 'X' as Fe, Ni, Ce & Co ions extracted from the raw materials like Ferric chloride, Nickel Nitrate, Cerium Nitrate & Cobalt Nitrate respectively. The preparation procedure was same as that of pure BT.

### ❖ *Method II:*

The compositions of the doped specimens can be represented by a general formula,  $\text{Ba}(\text{Ti}_{1-z}\text{X}_z)\text{O}_3$ , where X is Co, Fe and Ni with z = mole fraction. The polymer template in  $\text{Ba}^{2+}$  and Co/Fe/Ni doped  $\text{Ti}^{4+}$  cations arranged via PVA molecules was obtained by dispersing barium acetate, tetraisopropyle orthotitanate ( $\text{C}_{12}\text{H}_{28}\text{O}_4\text{Ti}$ ) and  $\text{Co}(\text{NO}_3)_2/\text{FeCl}_3/\text{Ni}(\text{NO}_3)$  in PVA as follows. First of all, a solution of ethyl alcohol and acetic acid in the volume ratio of 3:1 was prepared. Weighted amount of tetraisopropyl orthotitanate was hydrolyzed in that solution and the mixture (A) were stirred for 2h. Aqueous Solution of barium acetate (1.07 M) was poured into the First solution and the resulting mixture (B) was stirred for another 1h. The solution **B** was clear and transparent. In the Next stage, aqueous solution of cobalt nitrate / ferric chloride/ Nickel nitrate was added to the precursor **B**. Finally PVA (3 g/dl) was added to this solution drop-wise. Several processes of hydrolysis and polycondensation result in a polymer gel

at room Temperature. The gel was dried (in oven at 70 °C for 24 h) and calcined at 750 °C to crystallize the BT phase. In simple case, the decomposition reactions of the tetra-isopropyl orthotitanate in air can be expressed as



A similar reaction occurs in barium acetate,  $\text{Ba}(\text{CH}_2\text{COO})_2 \rightarrow \text{BaO} + 2\text{CO} + \text{H}_2$ . As an intermediate reaction product, the ethene gas  $\text{C}_2\text{H}_4$  reacts instantaneously with  $\text{O}_2$  (from the air), leading the precursor to encounter an autocombustion. In air, it occurs at temperature as high as  $\sim 400$  °C. Finally,  $\text{BaO} + \text{TiO}_2 \rightarrow \text{BaTiO}_3$  shows the growth of small sizes at 600 °C or at lower temperatures. Decomposing a metal ion-polymer complex facilitates presumably a reaction of as small BaO and  $\text{TiO}_2$  as molecular species. Heating at higher temperatures burns off residual carbon as  $\text{CO}_2$ .

## 2.3. Measurement techniques

### 2.3.1. Microstructure

#### 2.3.1.1. X-ray diffractogram

Here, X-ray diffraction (XRD) technique is used for material characterization as well as for detailed structural clarification. We extracted the following information from our x-ray powder diffractogram of various powder samples: (i) Quality and confirmation of the prepared samples, (ii) The interplaner spacing  $d$  of the reflections, (iii) The intensities of the reflections, and (iv) The unit cell dimensions and lattice type. In our case, calcined powders were characterized with respect to phase identification, phase quantity measurement, crystallite size determination and lattice parameter measurement, etc., by using X-ray diffractometer (Model PW1710,  $\text{CuK}_\alpha$  radiation,  $2\theta=3^\circ\text{-}130^\circ$ ,  $\Delta 2\theta=0.03^\circ$ ). The average grain diameter of the crystallites ( $D$ ) were calculated from X-ray diffraction peaks widths  $\beta$  ( $= \Delta 2\theta_{1/2}$ ) using Debye-Scherrer relation



$$D = \frac{0.9\lambda}{\beta \cos\theta}$$

Where  $\lambda$  is the wavelength and  $\theta$  is the angle of diffraction.

The typical XRD pattern for BT nanoparticles after heating a polymer precursor at low temperatures differ from the cubic, tetragonal, rhombohedral, hexagonal or orthorhombic (I/II) phases of BT. The proposed structure was obtained by fitting the observed  $d_{hkl}$  and calculated  $d_{hkl}$  values. The  $d_{hkl}$  was calculated by the relation

$$d = \frac{1}{\sqrt{\frac{h^2}{a^2} + \frac{k^2}{b^2} + \frac{l^2}{c^2}}}$$

Where  $h, k, l$  and  $a, b, c$  are both variable.

### Structural and Microstructural Analysis by Rietveld Method

For Rietveld analysis, the diffraction data were taken at room temperature on step scan mode with step size 0.03 and 5 sec per step. During all the experiments, the X-ray source was supplied a voltage of 35kV and 30 mA current. The peak shape was assumed to be a pseudo-Voigt (pV) function with asymmetry. The background of each pattern was fitted by a polynomial function of degree four.

#### 2.3.1.2. High Resolution Scanning Electron Microscope (HRSEM)

HRSEM is an essential analysing technique for exploring microstructures of materials. The particle size and morphology of BT nanocrystals were studied with a high resolution scanning electron microscope (HRSEM) of Carl-Zeiss of model Supra-40, with 10-20 kV accelerated voltage.



#### 2.3.1.3. High Resolution Transmission Electron Microscope (HRTEM)

The microstructure of the specimens was observed under Transmission Electron Microscope (TEM, Philips, Model-CM12). The nano-grains were chemically analyzed with Energy Dispersive Absorption (EDAX) spectra. For investigation under TEM the powder samples were



dispersed in an acetone medium by ultrasonic vibrator. The dispersed samples were placed drop-wise on a carbon coated Cu grid. After drying for a few hours these grids were placed inside the TEM.

## 2.3.2. Physical Properties

### 2.3.2.1. Electron paramagnetic resonance (EPR)

Here, Electron paramagnetic resonance (EPR) or electron spin resonance (ESR) spectroscopy is used to detect chemical species that have one or more unpaired electrons, such as inorganic free radicals or inorganic complexes possessing a transition metal ion. The EPR spectra were studied at an



X-band frequency ( $\sim 9.43$  GHz) with a Varian Associates spectrometer (Model No. 109) and the frequency of the resonant cavity was measured by a DPPH marker at  $g = 2.0036$ .

From the EPR spectrum the  $g$  values were calculated by the relation,  $g = \frac{2\pi fh}{\beta B}$ ;  $B$  is in mT.

### 2.3.2.2. Dielectric Properties

#### 2.3.2.2.1. Calcinations

The powders were calcined at different temperatures (detailed heat treatments are cited in the text) by an indigenous programmable laboratory tube furnace to obtain nc-BT powder. To study the phase formation behavior and reaction mechanism, as grown sample were calcined at different temperatures from  $700$  °C to  $1000$  °C for 2 hour in an alumina crucible at heating rate  $3-5$  °C per minute and then cooled in the furnace. The calcined powders were grinded by an agate mortar to avoid agglomeration of the particles and were used for the study of their phase formation as well as their physical characters.

#### 2.3.2.2.2. Nucleation and growth

Nucleation and growth describes the first-order phase transition from an atomically dispersed phase to a solid condensed phase. During the first stage of the transition fluctuations in the homogeneous, metastable parent phase result in the

appearance of small quantities of the new phase. The unfavourable process of creating an interface opposes the gain in energy through the reduction in super saturation of the parent phase, leading to a critical size of nucleus, above which the nucleic develop rapidly and irreversibly into the new phase.

#### 2.3.2.2.3. Pellet Preparation

After calcinations, the powders were grinded by an agate mortar to avoid agglomeration of the particles. To have a pellet of diameter 10 mm and thickness 1 mm, a cylindrical steal die of 10 mm was taken. Initially the die was kept in a highly viscous mobile oil to prevent it from rousting. Taking out from the oil, the die was cleaned with acetone. Just before putting the granules in the die for pressing, some hydrophobic stearic acid solution was used in the inner surface of the die to avoid sticking of the powder on the inner surface of the die. The granules were put in the die and the piston was slowly inserted into the cylinder. Then the die containing the granules were uniaxially pressed with a pressure of 5 bars in a hydraulic press. Before releasing the pressure from the die, minimum 1 minute time was given to minimize the stress on the pellet. After the pellet was formed the green density was measured from its external dimension. Then the pellets were sintered to study the dielectric response of the materials.

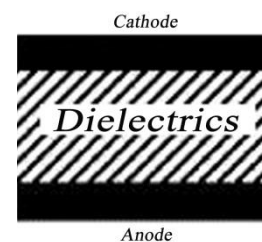


#### 2.3.2.2.4. Sintering

Density of the electronic ceramic is a very sensitive parameter and that directly affects their properties. Therefore, proper sintering of the pallets is essential for electrical measurement. The pellets were taken on an alumina plate and sintered at 1000 °C for 2 hours in a programmable furnace at a heating rate of 3-5 °C per minute. The pellets were furnace cooled and taken out of the furnace for initial density measurement. The porosity was found to be within permissible range.

#### 2.3.2.2.5. Electroding

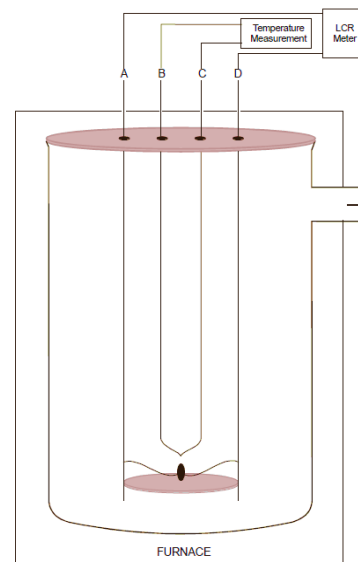
The selection of suitable electrode for the test materials is important. In our case, thin silver electrodes were printed on to opposite faces of the ceramic disk by screen printing technique. For organic removal printed disks were kept on an alumina plate



and first fired at 700 °C for 15 minutes. This procedure is repeated twice for better electroding.

### 2.3.2.2.6. Dielectric Permittivity

The capacitance of the sample was measured by using a LCR meter (Model 4284A, Agilent, Oswego, IL) in the range of temperature from 30 °C to 200 °C. A sample holder containing two copper leads separated at 10 mm apart inside a glass tube evacuated to a pressure level of  $10^{-3}$  Torr was used for the present case. The samples with 10 mm diameter and 1 mm thickness coated with silver paint (supplied by Acheson Colloiden B.V., Netherlands) on both the surfaces were connected to the copper leads of the sample holder. Finally the sample holder was inserted inside an oven whose



temperature could be controlled. The stray capacitance was subtracted every time to extract the correct capacitance values. The diagram of the sample holder is given in above figure.

### 2.3.2.3. Optical Properties

A Perkin-Elmer (Model-LS 55) Luminescence spectrometer in conjunction with a red sensitive detector (with gated photomultiplier with modified S5 response), with a pulsed xenon lamp (20 kW power with pulse width at half height  $<10\mu\text{s}$ ) as excitation source, was used to study the light emission from the samples. The data were obtained at a scan rate 100 nm/min, with variable entrance and/or emission slit width. The excitation source is a special



xenon flash tube, which produces an intense, short duration pulse of radiation over the spectral range of the instrument. A small festoon lamp close to the excitation source maintains an even triggering of the xenon flash tube. The Excitation and Emission monochromators can be scanned over their ranges independently, synchronously or driven to selected points in their ranges. Synchronous scanning can be either a fixed

wavelength difference or a fixed energy difference between the excitation and emission monochromators.

The spectral ranges of the monochromators are:

- Excitation monochromator 200 nm to 800 nm and zero order
- Emission monochromator 200 nm to 900 nm and zero order

The slit widths may be varied to give resolutions between 2.5 nm to 15 nm for the Excitation monochromator and between 2.5 nm to 20 nm for the Emission monochromator in increments of 0.1 nm. The value of 0 can also be selected for both the excitation and emission slit and this gives a resolution of  $< 2$  nm.

